TECHNICAL UNIVERSITY OF CLUJ-NAPOCA

ACTA TECHNICA NAPOCENSIS

Series: Applied Mathematics, Mechanics, and Engineering
Vol. 64, Issue III, September, 2021

MECHANICAL BEHAVIOR OF THE CARBON FIBRE REINFORCED PLASTICS

Adriana ŞTEFAN, George PELIN, Alexandra-Raluca PETRE, Monica MARIN, Cristina-Elisabeta PELIN, Sorina ILINA

Abstract: Composite materials based on carbon fibre reinforced plastics (CFRP) have gained importance for use in structural applications during the last few decades. In the present study, the tensile, flexural, shear, and comparison tests with numerical simulation are considered. The composites were obtained in the autoclave, and cured under controlled conditions, using a gradual increase of temperature. Test specimens were cut along two fiber directions, 0° and 90°, in order to compare the material behavior along these directions. The numerical simulation analysis was calculated using Nastran software. The microstructure was analyzed using optical microscopy and scanning electronical microscopy, observing the fractures, voids and fiber delamination.

Key words: *mechanical properties; morphology analysis; numerical simulation.*

1. INTRODUCTION

The use of composite materials in aviation industry is associated with Flyer 1 vehicle of Orvile and Wilbur Wright brothers, which was equipped with an Aluminum based engine in order to meet strength/weight ratio requirements. As a result, new and improved materials were needed for the aviation progress and ascended evolution. Therefore, composite materials, especially fiber reinforced composites (FRP) became of high importance for structural applications in the last decades [1-3], as their use led to new and improved properties. These properties improved the performance and operations of modern aircrafts, contributing to faster and lower costs worldwide travel. Last year's research confirms a continuous tendency of composite materials to evolve, through the improvement of development and processing of the existing materials in order to improve physical properties and/or to be able to use them in new domains and for them to have new employments for future applications. The appearance of new materials such as nanotubes and graphene are one of the factors that sustains the accelerated evolution and transformation of these materials and therefore sustaining the extension of their applications [3].

Composite materials were first used in military applications in aircrafts industry after World War II and their use extended nowadays in commercial aeronautics and aerospace [1]. Most composite materials exhibit superior strength compared with traditional metallic materials, generating weight reductions and decrease of fuel cost per passenger [2]. This attractive issue was one of the main reasons for aircraft manufacturers to desire the use of composite materials in the construction of the vehicles in their fleet.

As research and applications of fibers and matrix (both thermoset and thermoplastic) led to the obtaining of improved materials based on these components, resulting in carbon fiber reinforced composites (CFRP) with enhanced mechanical properties (the highest specific strength, stiffness and Young's modulus), that allowed the gradual replacement of conventional Aluminum and Titan alloys in primary structures. Although, CFRP were introduced in civil aviation in the '70s, thirty years were necessary to allow their use in primary structures [6, 7].

Received: 22.06.21; **Similarities**: 10.08.21: **Reviewed**: 20.07.21: **Accepted**:16.09.21.

Nowadays, the CFRP composites show an increased interest for aeronautical industry due to the newly discovered attractive characteristics of eco-friendly materials and behavior of smart materials [8].

In general, lightweight structures, like composite materials [4], provide increased payload, improved agility, short take-off, long-distance missions and high maneuverability.

Fibers such as carbon are increasingly common in the aeronautical and space industry, due to their high mechanical strength and low density. Carbon fibers are the perfect candidates for applications that require weight/resistance ratios and further weight reduction. The strength of the interfacial bond must be sufficient for the load to be transferred from the matrix to the fiber, if the composite is harder than the unreinforced matrix. Volume fraction plays a major role in determining the properties and it is considered the most important parameter to be taken into consideration for the influence of composite properties [8]. While technique and methodology for composite materials design are very well known, the knowledge and understanding of post-design issues remain long behind [5].

The mechanical behavior of glass and carbon fiber at different strain rates and temperatures was analyzed by C. Elanchezhian et al. [8], CFRP composite showing superior properties than GFRP in tensile and flexural loadings.

H. Koerber et al. [9] investigated the strain rate effect on unidirectional carbon-epoxy IM7 – 8552 in longitudinal compression. The dynamic experiment was designed by finite element analysis, using an axis-symmetric elastic model. They found that the longitudinal compressive modulus is not strain rate sensitive, but is dependent on the increasing of longitudinal compressive strength [9].

The effect of loading rate on fracture and mechanical behavior of cured glass fiber reinforced prepreg was studied by S. Sethi et al. [10] in an assessment of mechanical behavior and fractography study of glass/epoxy composites at different temperatures and loading speeds.

The report highlights that the interlaminar shear strength (ILSS) value is high at low loading speed and becomes low at high loading speed with the transition of loading rate at approximately 300 mm/min and the fracture starts to occur preferentially at fiber/matrix interface region [10].

The novelty of the problem is to emphasize, for the composite designers, the different results between the same types of materials but with different arrangements of the lamina layers, using different loading conditions. This aspect can indicate the appropriate technology that can be applied in the manufacture of the specimens, in order to obtain optimal results and performance in service of the materials.

The present paper presents the experimental analysis of CFRP specimens during different loads, in order to highlight the mechanical behavior of composites in different loading conditions.

Composite parent plates were obtained using autoclave process, and along with them during the same processing cycle, different specimen patches were developed. Two sets of patches were used to investigate the influence of strength and stiffness, as well as to understand load transfer from the parent board to the patches. Visual and acoustic inspections were used to follow the deterioration and failure process after the manufacture. The morpho structural analysis was performed through optical visualization and electronic scanning.

2. EXPERIMENTAL SECTION

2.1 Materials and obtaining procedures

Materials and specimens. The composite laminates for the parent plates were manufactured by autoclave using carbon fiber/epoxy prepreg M18/1 from Hexcel. The laminates had a stacking sequence [45/-45] and [0/90], which gives a quasi-isotropic property. Patches were made from the same prepreg but with different stacking sequences.

CFRP composite development process. The composite patches were obtained by direct curing using autoclave (SCHOLZ 442 Coesfeld L.W., upgraded in 2010). The pre-impregnated sheets of the material were impregnated under well-controlled condition (uniform fiber distribution, controlled fiber volume content and low void content) and cured using gradual temperature increase on the three-heating dwell

lapse of the oven with a temperature profile of 180°C. The prepreg sheets were cut with CNC cutter plotter and using Virtek device they were placed in the mold. Test specimens were cut along two fiber directions, 0° and 90°, in order to compare the material behavior along these two different directions.

2.2 Testing and characterization

Mechanical characterization. To evaluate the strength and stiffness the composites were subjected to mechanical testing (INSTRON 5982). Tensile, flexural, and interlaminar shear stress (ILSS) short beam shear (SBS) method tests were performed on a minimum of 5 specimen per test, according to SR EN ISO 527-4 at 5 mm/min tensile rate [11] for tensile, DIN EN ISO 14125 at 2 mm/min speed of test on rectangular specimens [12] for flexural and BS EN ISO 14130 at 2 mm/min speed of test [13] for SBS.

Morphological analysis. The morphological analysis was registered with optical microscopy (MEIJI 8520) and scanning electron microscopy (FEI - QUANTA 250 microscope) and it was performed in the fracture cross-section of the tested specimens to highlight the type of fracture and evaluate the matrix/fiber interface.

2.3 Numerical simulations

To better understand the use of the finite element method in order to reproduce the laboratory tests, the software MSC Patran was used and the analysis was computed using the linear static SOL 101 from MSC Nastran.

3. RESULTS AND DISCUSSION

3.1 Tensile Testing

Table 1 presents the average values of tensile stress and strain as well as Young Modulus of the specimens. The tensile test was performed for a set of 5 samples corresponding to each direction, 0 and 90 degrees respectively. The stress-strain curves recorded during the tensile test illustrated in Fig. 1 and Fig. 2, show a brittle behavior of the composite materials without any prior modification of elongation rate.

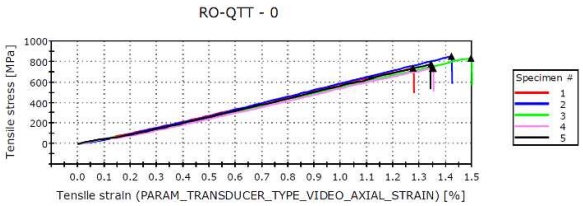

Fig. 1. Stress-strain curves during tensile tests of specimens cut in the 0° plane

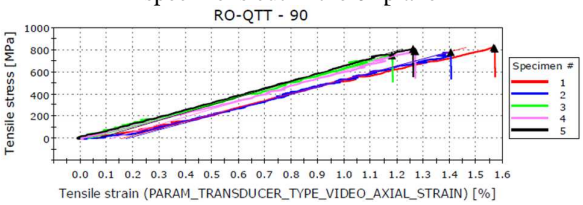

Fig. 2. Stress-strain curves during tensile tests of specimens cut in the 90° plane

Table 1

Mediated results of the tensile tested specimens

Sample	Load [kN]	Modulus [GPa]	Tensile stress [MPa]	Tensile strain [%]
0°	42,2	62,4	786	1,38
90°	42,4	66,3	787,1	1,33

As illustrated in Fig. 1 and Fig. 2 and shown in Table 1, there is a slight increase of the values mediated in the case of the samples cut in the 90-degree plane, which will be corroborated with optical microscopy.

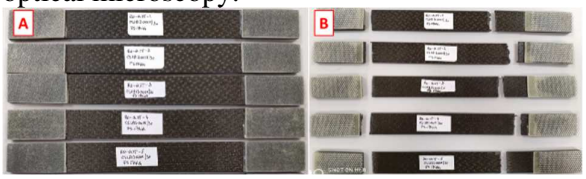

Fig. 3. Specimens in the 0° plane before and after and tensile testing

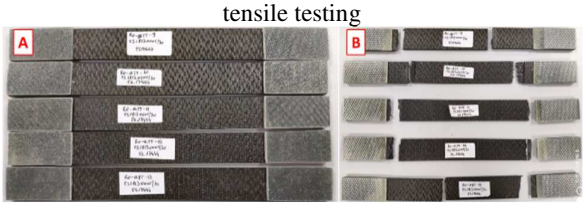

Fig. 4. Specimens in the 90° plane before and after tensile testing

Almost all 0° plane specimens presented the rupture location near the clamping tabs. In the case of 90° plane, some show breaking close to the clamping tables, while others broke at an appreciable distance from the tabs. All failure modes presented by the specimens have been considered valid, according to the testing standard and used for stress and Young's modulus calculation.

3.2 Flexural testing

All specimens tested at flexural loads fractured before reaching conventional deflection set according to the testing standard, this behavior being illustrated in the stress-strain curves shown in Fig. 5 and Fig. 6. This also indicates the brittle nature of the materials, which will further be investigated through the failure mode analysis achieved by optical and scanning electron microscopy techniques.

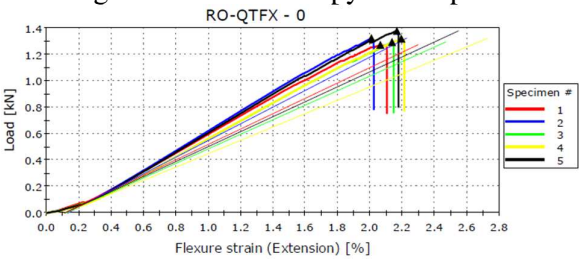

Fig. 5. Stress-strain curves during flexural tests of specimens cut in the 0° plane

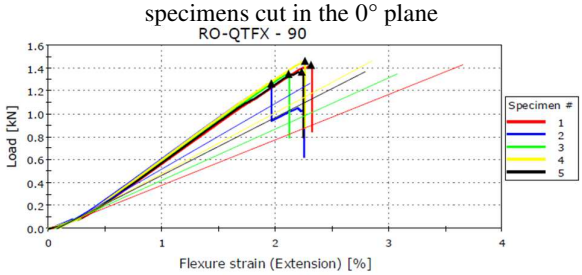

Fig. 6. Stress-strain curves during flexural tests of specimens cut in the 90° plane

Table 2

Mediated results of the flexural tests

Sample	Modulus [GPa]	Flexure stress [MPa]	Flexure strain [MPa]
0°	39,6	918,9	2,11
90°	34,9	986,5	2,18

As in the case of tensile test, also in the case of bending test, the samples cut in the 90-degree plane, show a slight increase in the average value of the bending resistance compared to those in the 0-degree plane, as it can be seen in the Table 2 and Fig. 5 and Fig. 6, respectively.

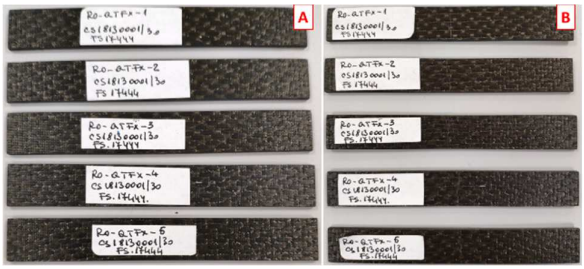

Fig. 7. Specimens in the 0° plane before and after flexural testing

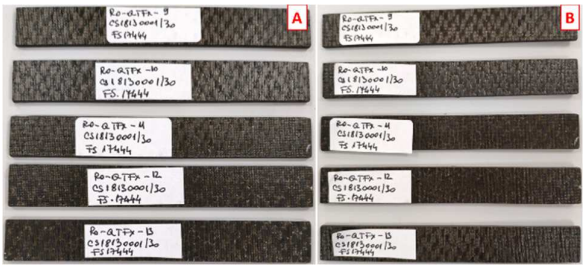

Fig. 8. Specimens in the 90° plane before and after flexural testing

3.3 Short beam test

For the short beam test, according to the testing standard, the specimens were loaded in a three-point bending arrangement, whereas an increase in the shear stress and interlaminar failure was realized by a suitable choice of the ratio of specimen thickness to the support span [12].

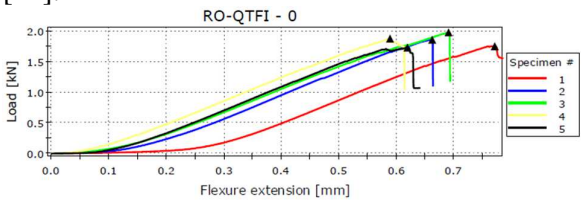

Fig. 9. Stress-strain curves during short beam shear tests of specimens cut in the 0° plane

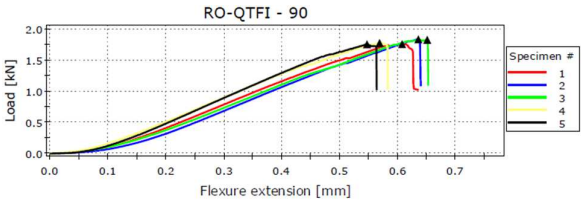

Fig. 10. Stress-strain curves during short beam shear tests of specimens cut in the 90° plane

Table 3

Mediated results of the Interlaminar shear strength

Sample	Apparent interlaminar shear strength [MPa]
0°	58,98
90°	57,94

In the case of short beam shear testing, apparent interlaminar shear strength was determined. The mediated results of the two sets of samples cut in the 90-degree plane and in the 0-degree plane have close values with minor differences between the two sets.

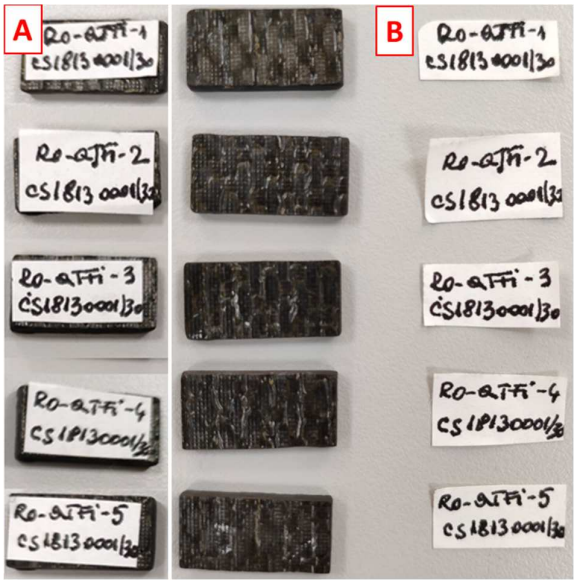

Fig. 11. Specimens in the 0° plane before and after short beam shear tests

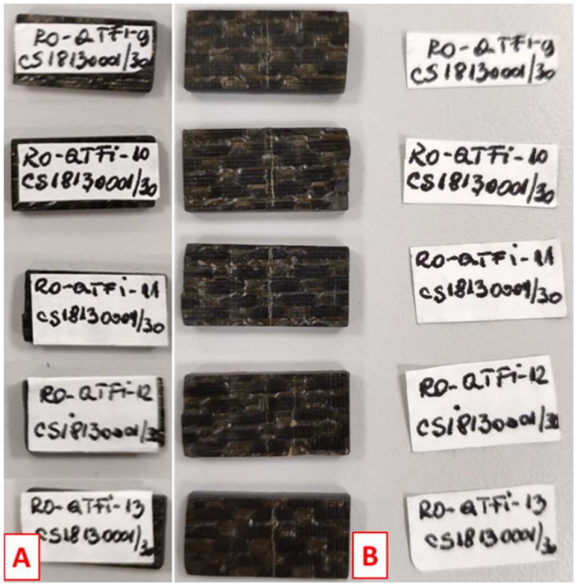

Fig. 12. Specimens in the 90° plane before and after short beam shear tests

Comparing the mechanical results for tensile, flexural and short beam tests with the information from the material datasheet [14], it can be observed that the differences are in the range accepted by the manufacturer.

3.4 Morphological analysis

All microscopical images were registered in the fracture area of the mechanically tested samples.

SEM and optical analysis were performed on the CFRP samples with the aim of visualizing the morphology which is characteristic to a fiber reinforced polymer laminated composite (Fig. 13 and Fig. 14) after testing, in order to visualize the morphology changes occurred in the tested material, and the interface between the two phases. Both techniques illustrate a clear visualization of the two phases that compose the laminated material, SEM providing supplementary detailed information that high magnifications offer.

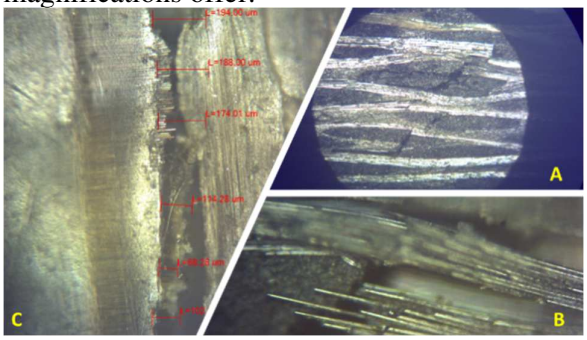

Fig. 13. Micrographs of carbon fiber fabric laminated composite with epoxy matrix and carbon fabric reinforcement (x2.5)

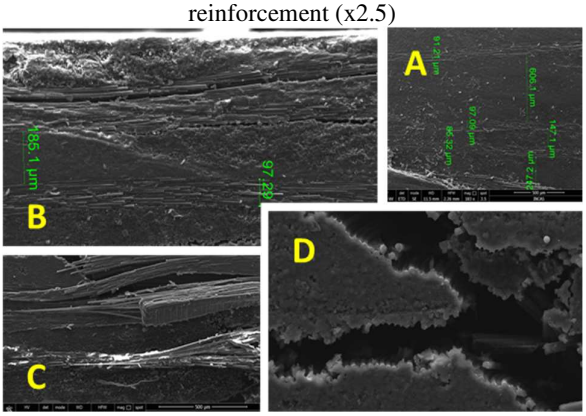

Fig. 14. SEM micrographs of carbon fiber fabric laminated composite with epoxy matrix and carbon fabric reinforcement (A – x183; B - x283; C – x283; D - x1131)

Optical micrographs of the specimens allow the visualization of the overall appearance of the samples, clearly showing the layered structure of the material (Fig. 13-A). Even low magnifications provided by optical microscopy allow the visualization of matrix microcracking (Fig. 13-A) and irregular distances between carbon fiber layers (Fig. 13-C), equivalent with non-uniform resin layers thickness. The observed issues were further investigated by SEM technique.

At different magnifications, SEM micrograph allows the visualization of layered structure of

the material (Fig. 14), allowing the analysis of high magnification details. The interface of the composite could offer valuable information about the adherence between reinforcement and matrix and could explain the mechanical behavior of the CFRP samples. The SEM images of the fracture surface of epoxy reinforced with carbon fiber fabric illustrate two different types of areas according to the matrix adhesion to the carbon fibers. Thus, one can observe areas in which the interface between the fabric and the matrix shows a proper mechanical interlocking, suggesting that a good interface was achieved in those areas.

It can also be observed that the distance between the plies varies, suggesting also different resin layers thickness, therefore a poor resin distribution. Based on the SEM image, the thickness of the carbon reinforcement is ranging between 85 μm – 97 μm, showing that the carbon layer is irregular. SEM micrographs illustrate areas were the resin detached from the fiber, suggesting a poor interface between the two phases. These issues were probably generated both by the pressing process during autoclave manufacture method, and also by the irregular fabric layers.

The SEM image also indicate some microcracking in the thermoset matrix and the main failure mode shown by optical micrograph is brittle for both fiber and matrix breakage which is specific to CFRP's. However, fiber breakage and matrix cracking occurred asynchronous. This failure mode indicates the poor interface between the two phases, showed also by the SEM images. This failure mode is frequently present in composites that exhibit poor resin distribution. In this case, probably the composite processing issues led to poor resin distribution that led to poor matrix-fiber interface, that consequently led to the described failure mode.

Nevertheless, analyzing the mechanical properties, it can be observed that the obtained values remain in the range accepted by the material datasheet [14], indicating that although the matrix-fiber interface exhibits areas that show adhesion problems, this issue does not generate a negative effect on the mechanical performance of the material. Thus, it can be assumed that probably the poor interface areas degree is significantly exceeded by the good interface degree that is able to ensure the proper mechanical load transfer within the composite, necessary to achieve suitable mechanical performance.

Future studies will take into consideration improving the obtaining process parameters control in order to achieve a strong interface on an extended level in the composite, providing strong reproductible results.

4. NUMERICAL SIMULATIONS OF THE MECHANICAL TESTS

In order to reproduce the laboratory tests, the software package MSC Patran/Nastran was used. The aim was to better understand the use of the finite element method and comprehend the behavior of this type of material for further use in the aerospace design of structures. The focus was on micro-scale analysis. The objective of the numerical simulation is to verify the validity of the micro-scale model in comparison with the experimental results.

The coupon modeled was composed of 9 layers of carbon fibre prepreg Hexcel M18/1 43%G939 Fabric. A laminated property PCOMP was created using a 2D orthotropic material MAT8 of each layer of 0.227 mm with the mechanical properties taken from the producer datasheet. Because each coupon has a different configuration, in order to catch the actual behavior of it, 2D element with edge length of 1 ÷ 2.5 mm was used.

The analysis was computed using the linear static SOL 101 from MSC Nastran and the results used for comparison are the minimum Strength Ratio for all plies by using the Tsai-Wu theory of Fibre Failure.

The load introduced for each analysis was the mean load at failure of the coupons from the results of the test. The results of the analysis are interpreted in terms of the failure behavior. The approaches are compared with the experimental results. For the unit cells, the strength ratio is predicted in order to characterize the failure behavior.

4.1 Tensile test

The main characteristics of the model of the tensile coupon are presented in Fig. 15. In Fig. 16 there are presented the results for minimum Strength Ratio of all plies, with a value of 0.97. The necking occurs at the exact point when the true strain at the maximum elongation and at the point when it reached the strain-hardening limit of the material.

4.2 Flexural test

The main characteristics of the model of the flexural in 3 points coupons are presented in Fig. 17. In Fig. 18 there are presented the results for minimum Strength Ratio of all plies, with a value of 0.78. The numerical results are close to the experimental results.

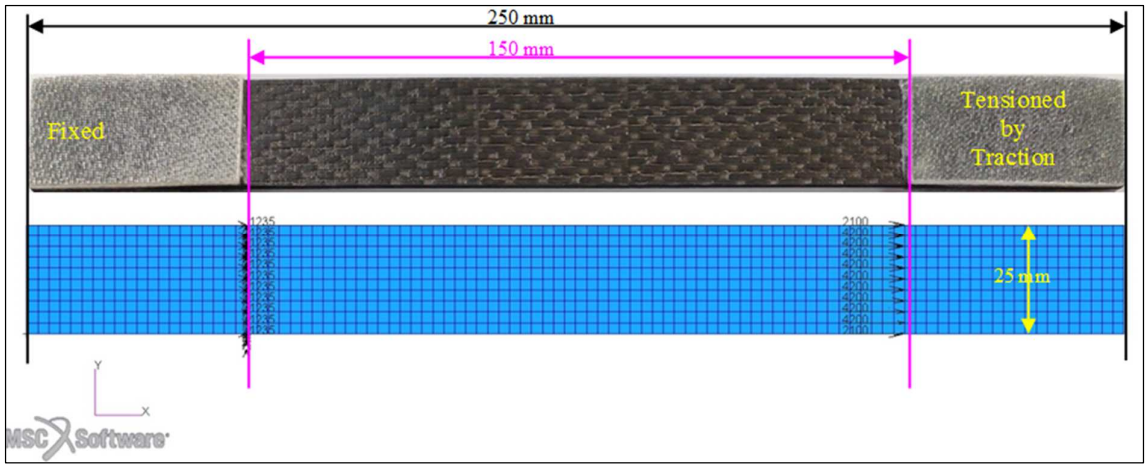

Fig. 15. The main characteristics of the model of the tensile coupon

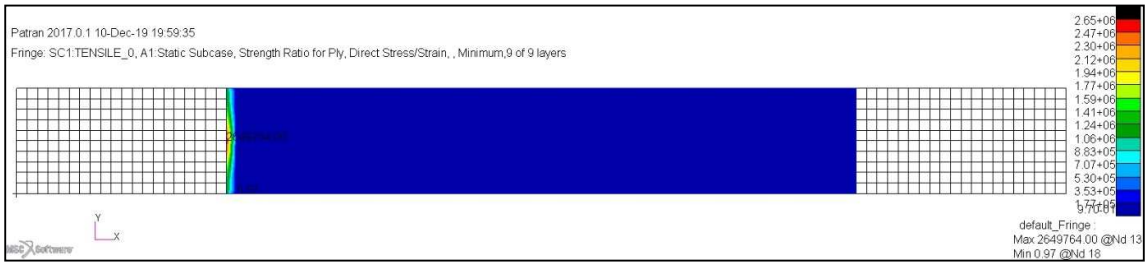

Fig. 16. The results for minimum Strength Ratio of all plies

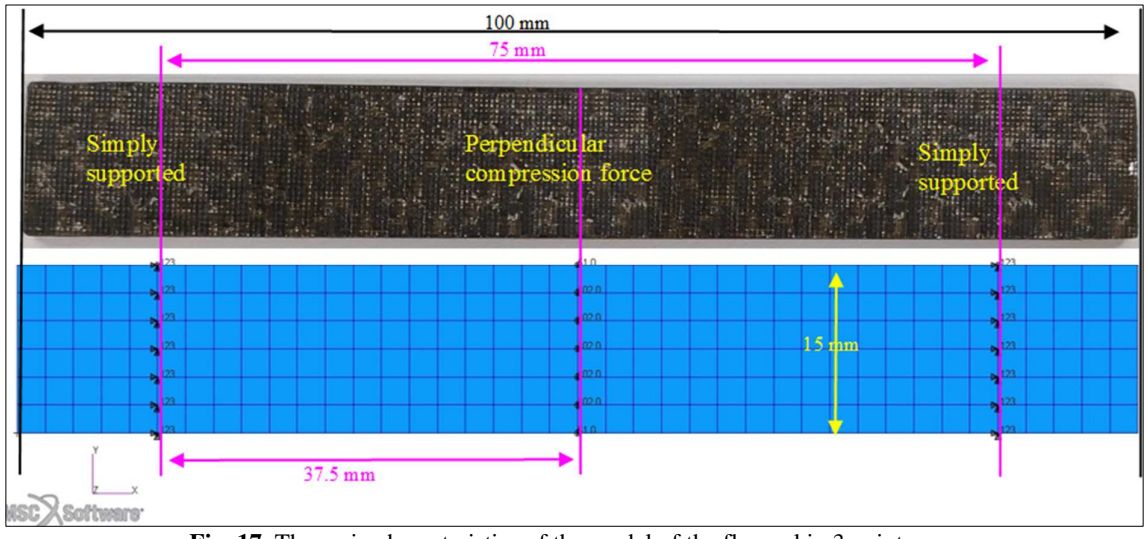

Fig. 17. The main characteristics of the model of the flexural in 3 points coupons

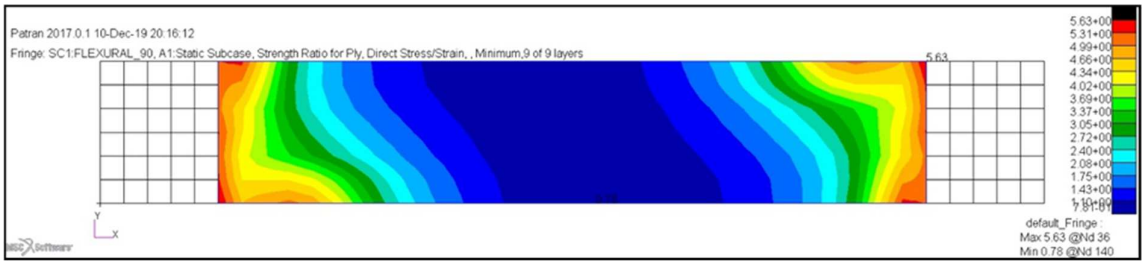

Fig. 18. The results for minimum Strength Ratio of all plies

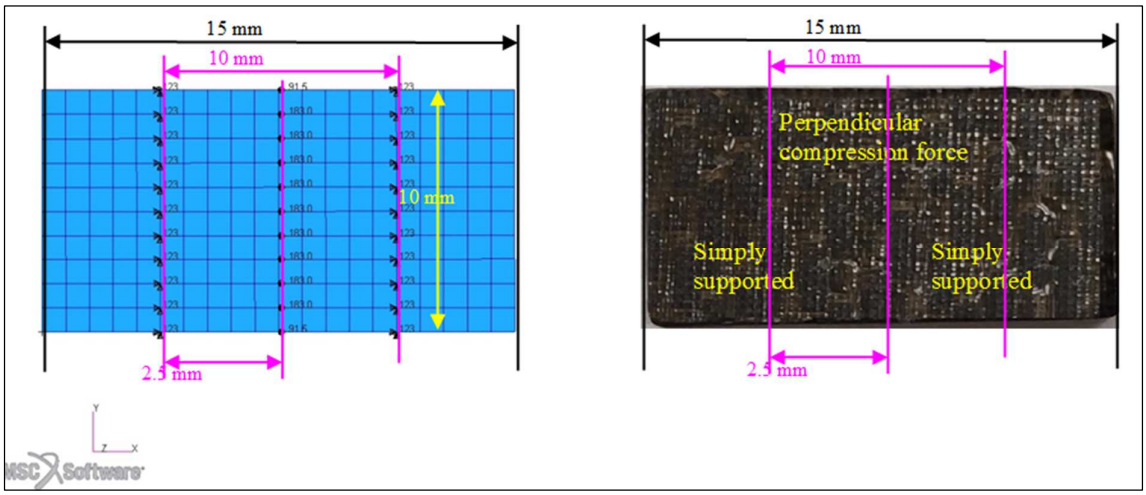

Fig. 19. The main characteristics of the model of the ILSS coupon

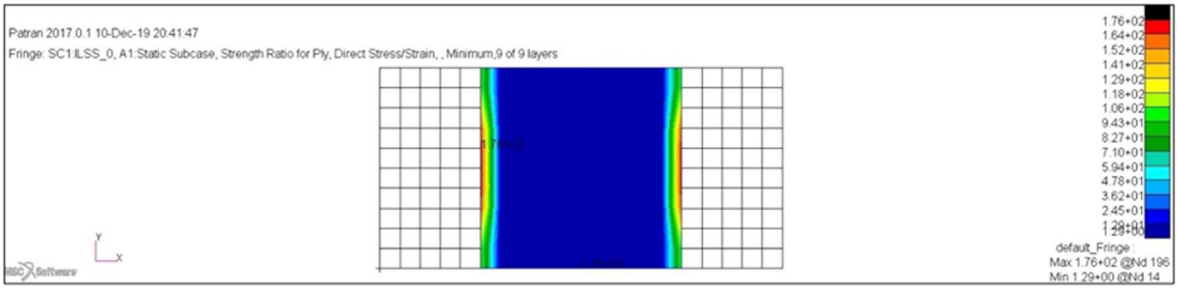

Fig. 20. The results for minimum Strength Ratio of all plies

4.3 Interlaminar shear strength (ILSS) test

The main characteristics of the model of the ILSS coupon are presented in Fig. 19.

In Fig. 20 there are presented the results for minimum Strength Ratio of all plies, with a value of 1.26. A discrete nodal displacement replaces the die that loads the specimen.

5. CONCLUSIONS

The results of the experimental study could be summarized in a few conclusions:

1. The study presents the mechanical behavior and numerical analysis of CFRP laminated, which were manufactured by autoclave.
2. The microscopic characterization of the CFRP included SEM microscopy as well as optical microscopy. Images obtained using both techniques showed that the interface between matrix and carbon fibre fabric could be subjected to improvement procedures, however the corroboration with mechanical test results indicates that the interface was good enough to obtain suitable mechanical properties values.

3. The microscopical investigations that were corroborated with the mechanical results and compared with numerical simulation provided a clearer image for the design process.
4. The prediction of failure behavior of CFRP was made by FE model. The simulation results show that the difference between tensile and flexural are due to the fact that the real thickness is different and maximum load for failure in the experimental test is slightly higher.
5. According to the mechanical properties in flexural strength case, the present study reveals the different results exhibited by materials with different arrangement of lamina layers and loadings conditions.

Also, comparing the properties obtained within the experimental tests with the properties shown in the material datasheet [14], it can be observed that the values of strength and modulus are in the same range, and there are no major variations.

Considering all these results, the analysis with FEM is reliable for aerospace structures and the laboratory test results offer the possibility to reduce the factors of safety in the stress analysis. The paper offers information for design process on the mechanical behavior in laboratory conditions corroborated with the predicted behavior in simulation conditions of laminated materials obtained from acknowledged raw material prepreg, accepted to be used in aeronautics applications.

6. ACKNOWLEDGMENTS

This work was supported by European Fund of Regional Development through Operational Program Competitiveness 2014-2020; project number 2/1.1.3 H/01.02.2018, within Action 1.1.3 Creating synergies with R&DI actions of the Framework Program Horizon 2020 of the European Union and other R&DI international programs. The content of this material does not necessarily represent the official position of the European Union or the Romanian Government.

7. REFERENCES

[1] dos Santos, D.G., Carbas, R.J.C., Marques, E.A.S., da Silva, L.F.M. *Reinforcement of CFRP joints with fibre metal laminates and additional adhesive layers*, Composite part B, vol. 165, 386-396 (2019)

[2] Mrazova, M. *Advanced composite materials of the future in aerospace industry*, INCAS Bulletin, vol. 5, iss. 3, 139–150, (2013)

[3] Kausar, A., Rafique. I., Muhammad, B. Aerospace *Application of Polymer Nanocomposite with Carbon Nanotube, Graphite, Graphene Oxide, and Nanoclay*, Polymer-Plastics Technology and Engineering, vol. 56, iss. 13, 1438-1456, (2017)

[4] Hegnell, M.K., Akermo, M. *A composite cost model for aeronautical industry: Methodology and case study*, Composite part B, vol. 79, 254-261, (2015)

[5] Åström, B.T. *Manufacturing of Composite Polymers*, Nelson Thornes Ltd, Stockholm, Sweden, 92-95, 2002

[6] Hallander, P. *Compraser Composite Course -Material and manufacturing*, Stockholm, Sweden, 2007

[7] Soutis, C. *Carbon fibre reinforced plastic in aircraft construction*, Materials Science and Engineering. A vol. 412, 171-176, (2005)

[8] Elanchezhian C, Vijaia Ramnath, B. Hemalatha, J. *Mechanical behavior of glass and carbon fibre reinforced composites at varying strain rates and temperatures*, 3rd international Conference on Materials Processing and Characterization (ICMPC 2014), Procedia Materials Science vol. 6, 1405 – 1418, (2014)

[9] Koerber, H., Camanho, P.P. *High strain rate characterization of unidirectional carbon-epoxy IM7-8552 in logitudinal compression*, Composite Part A: Applied Science and

Manufacturing, vol. 42, iss. 5, 462-470, (2011).

[10] Sethi, S., Chandra Ray, B. *An assessment of mechanical behavior and fractography study of glass/epoxy composites at different temperatures and loading speeds, Materials and Design*, vol. 64, 160-165, (2014)

[11] Standard Test Method for Tensile Properties of Polymer Matrix Composite Materials (DIN EN ISO 527-4)

[12] Determination of apparent interlaminar shear strength by short-beam method (DIN EN ISO 14130)

[13] Determination of flexural properties (DIN EN ISO 14125, Class IV)

[14]. M18/1 Prepreg Datasheet

Compartamentul din punct de vedere mecanic al materialelor plastice ranforsate cu fibre de carbon

Materialele compozite pe bază de materiale plastice ranforsate cu fibre de carbon (CFRP) au devenit tot mai importante pentru aplicaţii structurale în timpul ultimelor decenii. În studiul prezent au fost luate în considerare teste de tracţiune, încovoiere şi forfecare şi comparaţia lor cu simulările numerice. Compozitele au fost obţinute în autoclave, prin reticulare în condiţii controlate, folosind o creştere graduală a temperaturii. Epruvetele de testare au fost tăiate de-a lungul a două direcţii, 0° şi 90°, în vederea realizării unei comparaţii între comportamentul materialului de-a lungul acestor direcţii. Analiza de simulare numerică a fost efectuată utilizând softaware-ul Nastran.Microstructura a fost analizată cu ajutorul microscopiei optice şi microscopieie electroncie de baleiaj, observând-se fisurile, golurile şi delaminarea fibrelor.

Adriana ŞTEFAN, Phd Phys, Scientific Researcher I, National Institute for Aerospace Research "Elie Carafoli" – I.N.C.A.S, Materials and Tribology Unit, stefan.adriana@incas.ro, 220 Iuliu Maniu Blvd, 021126, Bucharest, Romania

George PELIN, Phd Chem Eng, Scientific Researcher III, National Institute for Aerospace Research "Elie Carafoli" – I.N.C.A.S, Materials and Tribology Unit, pelin.george@incas.ro, 220 Iuliu Maniu Blvd, 021126, Bucharest, Romania

Alexandra-Raluca PETRE, Eng, Scientific Researcher III, National Institute for Aerospace Research "Elie Carafoli" – I.N.C.A.S, Materials and Tribology Unit, petre.alexandra@incas.ro, 220 Iuliu Maniu Blvd, 021126, Bucharest, Romania

Monica MARIN, Eng., ROMAERO S.A, monica.marin@romaero.com, 14 Ficusului Blvd, 013975 Bucharest, Romania

Cristina-Elisabeta PELIN, Phd Chem Eng, Scientific Researcher III, National Institute for Aerospace Research "Elie Carafoli" – I.N.C.A.S, Materials and Tribology Unit, pelin.cristina@incas.ro, 220 Iuliu Maniu Blvd, 021126, Bucharest, Romania

Sorina ILINA, Phys, Scientific Researcher, National Institute for Aerospace Research "Elie Carafoli" – I.N.C.A.S, Materials and Tribology Unit, ilina.sorina@incas.ro, 220 Iuliu Maniu Blvd, 021126, Bucharest, Romania